TAPP, ANNA F., M.A. Mapping the Impact of Vegetation and Terrain on Cellular Signal Levels. (2008)
Directed by Dr. Rick L. Bunch. 60pp

The purpose of this research is to look into the impact that rough topography combined with dense vegetation can have on a digital cellular phone signal. The research area is the Deep Creek region of the Great Smoky Mountains National Park. In addition to hosting an unmatched amount of biological diversity for its acreage, the Great Smoky Mountains National Park is the most visited U.S. national park.

A classified vegetation map of the park was obtained from the National Park Service. An all returns LIDAR dataset was used to create a terrain model and a tree canopy model. Field measurements were conducted in both leaf on and leaf off conditions along the trails of the Deep Creek region, located north of Bryson City and south of Clingman's Dome.

Significant relationships were found relating soil moisture and tree heights to attenuation. Soil moisture was found to have a significant impact on the leaf on v. leaf off difference. The height of the tree canopy was a more significant contributor to attenuation than the species of the tree. In this study the species of tree was only significant insomuch as it was an indicator of the tree height.

MAPPING THE IMPACT OF VEGETATION AND TERRAIN ON CELLULAR SIGNAL LEVELS

by

Anna F. Tapp

A Thesis Submitted to
the Faculty of The Graduate School at
The University of North Carolina at Greensboro
in Partial Fulfillment
of the Requirements for the Degree
Master of Arts

Greensboro
2008

Approved by

_____
Rick L. Bunch, PhD, Committee Chair

APPROVAL PAGE

This thesis has been approved by the following committee of the Faculty of The Graduate School at The University of North Carolina at Greensboro.

Committee Chair _____
Rick L. Bunch, PhD

Committee Members _____
Roy S. Stine, PhD

_____
Robert Y. Li, PhD

April 11, 2008
Date of Acceptance by Committee

April 4, 2008
Date of Final Oral Examination

ACKNOWLEDGEMENTS

Thanks to Dr. Rick Bunch for his perpetual assistance and expertise. Thanks to CityScape Consultants, Inc. for their technical guidance. A special thanks to Stephanie Jane Edwards, Kirsten Hunt and Kay Miles for their hours of hiking through the woods. Finally, none of this would have been possible without the help of Andrew Tapp, my support team and permanent field partner. The field work was funded by the Center for Geographic Information Science and Health at the University of North Carolina at Greensboro.

TABLE OF CONTENTS

Page

LIST OF TABLES

Page

LIST OF FIGURES

Page

CHAPTER I

INTRODUCTION

Over the last decade the world has experienced an explosion in cellular phone technology and innovation. In 1995, the number of cellular phones in the United States was 28 million. In 2001, the estimate was 118 million. In 2007 the numbers rose to 243 million subscribers (CTIA 2007). With this growing popularity, a demand has developed for access to information and communication at all times. Some view their cellular phones purely as recreational tools, while many others take comfort in the possession of mobile technology as a safeguard. Even the individual who does not regularly use a mobile phone may carry it with them "just in case." The assumption is that the technology will be fully functional when the user has a need. With over 210,000 cell phone tower sites in the country, that assumption is often a reality (CTIA 2007). Whether for convenience or for emergency, the interest is greater now than ever before to accurately predict when and where one can make a call. Engineers are collaborating with geographers to develop these prediction models quickly and accurately.

As individuals became increasingly dependent on mobile technology, the Federal Communications Commission (FCC) was forced to keep pace with innovation. In 1996 the FCC recognized the growing popularity of cellular communications when it passed rules establishing Enhanced 911 (E911). E911 was divided into two phases. In the first phase, wireless providers were required to report the phone number of callers dialing 911

along with the location of the antenna that handled the call. In the second phase, wireless providers were required to have the ability to transmit the location of a caller with an accuracy of fifty to three hundred meters (FCC 2000). Wireless providers had until September of 2003 to completely satisfy both phases of E911 (FCC 2005). Five years later, with positioning technology now firmly embedded in the cellular world, cell phone users have begun to take E911 for granted.

In the last several years, research has flooded the communications engineering world related to signal transmission in urban environments. Meanwhile stories continue to be published in the media related to rural accidents in which there was no cellular tower in range. *USA Today* wrote that in August 2007 alone, four separate hiking incidents made headlines (Copeland 2007). In one incident, hikers in New Jersey were able to use a cell phone to get help from the police. Others were not so lucky. In Oregon two hikers had to remain trapped for days in the wilderness before being reported missing by a concerned employer. Even the best wireless positioning technology is of no use unless there is an antenna to receive both the location signal and the call for help. Therefore the need to accurately predict radio frequency transmission is important not only in the urban environment, but also in the rural context.

The problem of weak cellular coverage in parks is a sensitive issue for many nature-lovers. As much as hikers would enjoy the security of cell phone coverage on their journeys, the existence of cell phone towers inside a preserved park impairs the natural landscape. Therefore if towers are to be placed inside or close to preserved parks, their numbers would have to be minimized and their appearances camouflaged as much

as possible. In order for the number of towers to be minimized, a volume of research is important to predicting the behavior of the signal in a densely forested environment.

The purpose of this research is to look into the impact that rough topography combined with dense vegetation can have on a digital cellular phone signal. The hypothesis is that radio signal field measurements in densely vegetated areas will be weaker than predicted values. If the hypothesis is confirmed, the subsequent goal is to determine how different environmental variables impact signal loss to different degrees. The research area is the Deep Creek region of the Great Smoky Mountains National Park. In addition to hosting an unmatched amount of biological diversity for its acreage, the Great Smoky Mountains National Park is the most visited U.S. national park, with eight to ten million visitors each year (NPS 2007). The National Park Service credits its popularity to its central location on the East Coast as well as its situation at the end of the Blue Ridge Parkway. Approximately one hundred and twenty-nine incidents occur in the park annually (NPS 2007), including at least one accidental fatality (Fraser 2002).

Five sets of data are vital in the consideration of this research problem:

- Cell phone tower sites,
- Terrain elevation grid,
- Vegetation height grid,
- Vegetation classification data,
- And a baseline pathloss prediction.

Each data set adds a vital layer to the analysis of radio frequency signal loss.

CHAPTER II

CELLULAR PHONE COVERAGE MODELING

Cellular phone technology is based on the concept of dividing the landscape into coverage cells typically three miles in diameter. Each cell can handle from five to fifty calls simultaneously (Molish 2005). Each provider is granted a limited amount of bandwidth by the FCC. By dividing and sub-dividing the landscape into cells, wireless providers are able to continuously increase capacity while maintaining the same small amount of bandwidth. Since each tower only transmits across a limited distance, frequencies can be reused by non-adjacent cells without causing destructive interference.

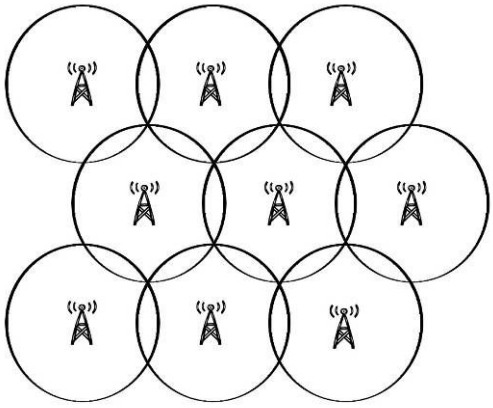

Figure 2.1. Ideal Cellular Network

The network is purposely designed so that each cell overlaps in part with multiple others (see Figure 2.1). The overlapping sections are referred to as "handoff zones". If

the user is in motion and passes through a handoff zone, one tower will take over for the next in a seamless transition. The user can be traveling as fast as 150 km/hr (92.5 mi/hr) and never know he or she is being handed from one tower to another (Molish 2005).

When determining the range and effectiveness of a cellular antenna, researchers calculate the path loss (also called attenuation) of the wave as it travels through space. Calculations are made using either milliwatts or decibels with respect to milliwatts (dBm). Results are often reported in dBm's, a convenient logarithmic unit. Free space loss is the amount of fading a radio wave will experience in a perfect, clutter-free environment (Rappaport 2002). Shown in Equation 2.1, free space loss can be derived mathematically.

$$\text{Friis Free Space Equation} \qquad \Pr(d) = \frac{P_r G_t G_r \lambda^2}{(4\pi)^2 d^2 L} \qquad (2.1)$$

$P_r(d)$ = received power (mW) as a function of distance
d = distance in m
P_t = transmitter power (mW)
G_t = transmitter gain (unitless)
G_r = receiver gain (unitless)
L = system loss factor

Since such a perfect environment does not exist in experience, practical formulas used to predict path loss in the real world are empirical in nature. Each formula has been derived and refined through repeated field tests. The results of field tests are plotted and a fitted curve generated. The equation of the curve is published along with the appropriate frequency range and environmental situation under which it can be reliably applied. Empirical equations have been generated and refined to reflect the amount of loss that

will be generally experienced in urban and suburban environments at various frequencies (Hata 1980; Walfisch and Bertoni 1988).

$$L = 46.3 + 33.9 \log f - 13.82 \log h_B + [44.9 - 6.55 \log h_B] \log d - C_H + C \quad (2.2.1)$$

$$C_H = 3.2 [\log (11.75\, h_B)]^2 - 4.97 \quad (2.2.2)$$

L = path loss in dbm
f = frequency in MHz
d = distance in km
h_B = antenna (base station) height
C = 0 db for medium and suburban, 3 db for for urban

Where f is between 1500 and 2000 MHz, receiver height is up to 10m, base station antenna height is 30 to 100m and distance between receiver and antenna is up to 20km, and ground clutter is open, urban or suburban.

Equations 2.2.1 and 2.2.2 are the COST-231 formula, which is applicable in urban and suburban areas with frequencies between 1500 and 2000 MHz (Walfisch and Bertoni 1988).

The major drawback to this type of model is the assumption that the ground cover across one's entire area can be classified uniformly. In the example of the COST-231 model, C (known as the clutter value) is a constant. When used in application, the COST-231 suggests one of two C values for urban or suburban.

GIS has the capacity for making this type of calculation more robust with the entrance of land cover classes. Publicly available land cover datasets can be used to differentially calculate the path loss across the coverage map. Within the same map areas classified as urban can be calculated differently than areas classified as suburban.

The incorporation of geospatial datasets has produced an impetus to move beyond these average empirical formulas to more precise propagation calculations. Researchers

are increasingly interested in quantifying to what extent more specific forms of ground clutter interfere with the signal. For example, how does a wooden structure interfere with the signal compared to a concrete structure? Given this kind of information, the "urban" class can be broken down into innumerable sub-categories, each with its own clutter value. As technology and research progresses, the goal is to create a model that begins with a free space calculation and from there adds each known variable, from weather to building materials to vegetation types, to produce increasingly accurate path loss predictions.

Rubinstein took a step in this direction in his 1998 research. He overlaid Land Use Land Cover (LULC) data over his measurement points. He calculated the difference between measured and predicted values for three separate band-widths. The differences within each LULC class were averaged to arrive at an estimated clutter value for each class located within the research area. Although this study takes a strong step by using national geospatial data to predict signal strength, the choice of using the LULC dataset for this application was slightly problematic. A radio wave is impacted most by the physical nature of the land cover and not by the way the land is being used. For example, LULC distinguishes between a lake or reservoir, and industrial or commercial. The behavior of a radio signal will be no different based solely on the cultural usage of a body of water or building. There can also be wide land cover variations within land use categories that could throw off the results, especially in urban and suburban applications.

Existing research has primarily focused on urban and suburban areas, where most of the cellular customers reside. A smaller body of research has attempted to pinpoint the

impact of vegetation on wave attenuation. These studies unanimously agree that vegetation has a strong impact on the fading of a radio wave (Vogel and Goldhirsh 1986; Tewari, et al. 1990; Goldman and Swenson 1999; Dal Bello, et al. 2000). Unlike research conducted in urban environments, there have been limited attempts to quantify the impact of various forms of vegetation.

One such attempt was made in 2002, at the behest of the United Kingdom Radiocommunications Agency. The company QinetiQ attempted to create a generic model of propagation through vegetation. In their research, they used five specific types of trees as benchmarks – sycamore, silver maple, London plane, horse chestnut and common lime. The excess loss as a wave passes through these types of trees (or trees with similar leaf sizes and leaf area indices) can be calculated under this paradigm. Unfortunately its application is limited to environments with similar tree types and no undercanopy. Additionally, this study made no attempt to measure differences between leaf on and leaf off situations.

The door is open for further investigation into the impact of vegetation on the fading of radio waves. Past research has been limited to one or few vegetation types per study. The National Park Service has completed a massive vegetation classification project for the Great Smoky Mountains. The dataset divides this region into forty classes of over and undercanopy. This detailed classification scheme combined with the vegetative diversity of the area makes it an ideal location for research focusing on vegetation native to the United States.

CHAPTER III

TERRAIN AND CANOPY MODELING

Line of Sight Calculations

In addition to free space attenuation, other factors impact signal strength across space. Without line of sight or near line of sight access to an antenna, the cellular phone will not receive a signal, regardless of its distance to the transmitter. The GIS viewshed has been adopted as the logical first step for predicting where radio waves can physically reach. The goal of the viewshed is to classify each elevation model cell as either visible or invisible from a predefined vantage point (see Figure 3.1).

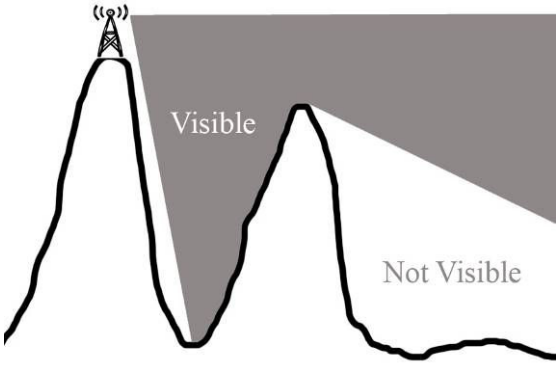

Figure 3.1. Viewshed Classification

The principle of viewshed analysis is to look at each intermediate cell between the observation point and the destination point and to determine the elevation slope. If the slope between the source and an intermediate cell is greater than the slope between the

source and the destination, then the view must be at least partially blocked (Sorenson and Lanter 1993). Either a raster or vector model can be used in such an analysis.

Light Detecting and Ranging (LIDAR) data has been increasing in popularity as an alternative to the photogrammetrically-derived USGS DEMs. A LIDAR system mounted on an aircraft will measure the time it takes a pulse of laser to hit the earth and return backscatter. The more laser pulses emitted from the aircraft, the higher the resolution of the subsequent elevation model. The USGS photogrammetrically-derived topographic maps claim a vertical accuracy of half of one contour interval (5 feet for 10-foot contour lines) for 90% of the points surveyed (USGS 2006). In contrast, LIDAR-derived DEMs boast accuracies as small as 7 cm (NCFM 2003).

In addition to its high accuracy level, another benefit of this technology is its ability to measure both ground and canopy heights simultaneously. As the scanner measures the backscatter of the laser pulses, multiple returns from the same laser pulse will indicate multiple levels of ground cover. The first return reflects the elevation of the top of the canopy, while the last return generally indicates the ground elevation (Roberts et al. 2004; Hyde et al. 2006). There will also be last returns which never reach the ground, bouncing off buildings, tree trunks, and other ground clutter. These points can be differentiated from ground points using filtering algorithms.

Several filtering algorithms have been proposed to eliminate false ground readings. Most operate on the conservative premise that since these scanners are so prolific in their number of returns, throwing out some good returns along with the outliers is better than leaving outliers in the dataset. Since wooded areas have an abundance of

problematic points above the ground, the result can be the removal of most of the points by the end of the filtering algorithm.

In the filtering process, both falsely high and falsely low readings must be eliminated. Falsely high elevation values are largely due to canopy obstructions. Falsely low elevation values are a result of multipath. If part of the emitted energy bounces between surfaces before returning to the scanner, the scanner will calculate a value that actually lies below the earth's surface.

Most filtering algorithms are based on the principle that drastic height changes between two relatively close LIDAR points are suspicious. Some algorithms use slope as a measure (Zhang et al. 2003; Zaksek and Pfeifer 2006; Kilian et al. 1996). Others use the principle of linear prediction, in which strong outliers are iteratively removed until a good approximation of the ground is obtained (Kraus and Pfeifer 1998). Yet another group of methodologies involves segmentation of the terrain. Using region growing principles, the LIDAR point cloud is divided into segments representing various terrain and canopy elements such as buildings, trees and ground. The assumption is that, at the end of the procedure, the largest segment must be the ground (Jacobsen and Lohmann 2003; Verma et al. 2006). A few years ago Sithole and Vosselman set out to evaluate various algorithms. They discovered that the segmentation method was most robust (2004). However they concluded that in wooded areas with steep terrain all the algorithms tended to fail, including segmentation.

Kobler et al. chose to develop an algorithm suited to wooded areas with steep terrain (2007). Their resulting technique is called repetitive interpolation (REIN). First

the strongly positive and negative outliers are removed from the data. Citing previous research showing that an intelligent analyst can remove outliers through simple observation (Sithole and Vosselman 2004), they recommend visually removing the obvious errors. To remove additional outliers, the slope between each point and its nearest neighbor is calculated. Those points with slopes significantly higher than the steepest slope expected in the area are eliminated. In the final filtering stage, independent random samples are taken from the LIDAR data. An elevation model is created from each sample. The result is a distribution of elevations at each location in the model. Since LIDAR data is most plagued with positive canopy outliers, the lowest elevation at each point is assumed to be closest to the truth. An adjustment value called the global mean offset (*gmo*) is calculated based on the differences between the independent random sample interpolations. The *gmo* is added to the minimum elevation at each point to determine the elevation value of the final output terrain model (Kobler et al. 2007).

Whatever the algorithm used to determine the ground elevation points, a choice must be made about the spatial resolution of the output DEM. A balance needs to be struck between the necessary accuracy and the processing time. The more points included in the interpolation, the greater the accuracy and the longer the processing time. Anderson et al. proposed solutions for determining the best mix of accuracy and data reduction (2006). In their study they performed random data reduction methods. After each data reduction and subsequent interpolation, they compared the output to a DEM created from the entire set of points. They show that a 5-meter DEM with about 143 data points per hectare (representing 50% of their original dataset) will not be statistically

different from a 5-meter DEM created from 100% of the points. On the other hand, only 40 data points per hectare would be necessary (10% of their original dataset) to create a similar 30-meter DEM. Anderson et. al. showed that it is valid to randomly select a portion of the entire dataset to create a DEM in a fraction of the time.

Tree Canopy Model

Using all returns LIDAR data, it is possible to create an elevation grid representing the ground in addition to a grid modeling the upper tree canopy. Such grids are typically made through linear interpolation of the LIDAR points, potentially yielding a vertical accuracy as small as 0.5 m (Roberts et al. 2004; Hyde et al. 2006). This technique is best employed with LIDAR collected in leaf on conditions. It remains to be seen if leaf off LIDAR could produce a canopy model approximating the ground truth.

The benefit of a canopy model for this research would be the incorporation of a new independent variable – distance through ground clutter. In the past, the vegetation ground clutter values used in propagation algorithms have been absolute numbers (Rubinstein 1998). Some work has been done testing construction materials for determining building penetration (Rappaport 2002), however this type of research has not yet been widely extended to rural features like forests. Schwering et al. made some observations of which frequencies better penetrate vegetation (1988), but made no inferences that could be incorporated into a robust computer model.

If GIS could be used to model the distance traveled through the vegetation canopy, research could determine clutter in terms of dBm's lost per meter. The

assumption is that the attenuation of the wave should be less severe on the edge of a forest than several meters into the forest (Schwering et al. 1988). Modeling the canopy cover would produce new opportunities to examine radio wave behavior.

Diffraction Estimates

Unfortunately line of sight using the viewshed analysis does not give a complete picture of cellular coverage. Diffraction not only allows radio waves to travel across the curved surface of the earth, but it also gives radio waves the ability to propagate around obstacles to some extent. These areas outside the line of sight are called "shadowed." The signal strength will rapidly decrease in these shadowed regions, but often enough useful signal will still remain (Rappaport 2002). Some simple situations can be calculated, among which are knife-edge diffraction and multiple knife-edge diffraction (Deygout 1966; Bullington 1947; Epstein and Peterson 1953). Signal strength approximations can be made from these cases and applied to a propagation model.

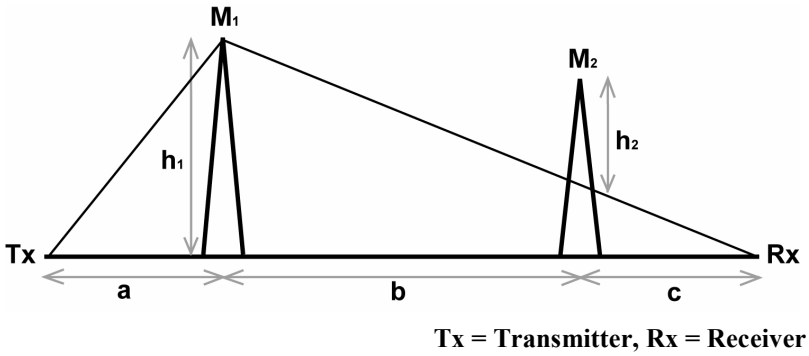

Figure 3.2. Multiple Knife-Edge Diffraction

One of the most widely-used diffraction algorithms was described by Deygout in 1966. He presented a formula that could be used iteratively for multiple obstructions. Figure 3.2 shows an example of two obstructions. Deygout's method is to first compute the diffraction loss of the main obstacle (path TxM_1Rx in Figure 3.2). The next step is to compute the secondary diffraction loss by applying the same calculations to the path M_1M_2Rx. Those loss values are added together. Finally, a correction factor is incorporated into the equation, completing the total diffraction loss calculation (*TDL*).

$$TDL = ML + SL - TC \tag{3.1.1}$$

$$ML = 20\log\left(h_1 / r_1\right) + 16 \tag{3.1.2}$$

$$\text{where } r_1 = 548\sqrt{a(b+c) / f(a+b+c)} \tag{3.1.3}$$

$$SL = 20 \log \left(h_2 / r_2 \right) + 16 \tag{3.1.4}$$

$$\text{where } r_2 = 548\sqrt{c(a+b) / f(a+b+c)} \tag{3.1.5}$$

$$TC = \left(12 - 20\log\left(\frac{2}{1-\alpha/\pi}\right)\right)\left(\frac{q}{p}\right)^{2p} \tag{3.1.6}$$

$$\text{where } \tan\alpha = \sqrt{\frac{b(a+b+c)}{ac}} \tag{3.1.7}$$

$$\text{where } q = \frac{h_1}{r_1}\sqrt{2} \text{ and } p = \frac{h_2}{r_2}\sqrt{2} \tag{3.1.8}$$

f = frequency of the signal
λ = wavelength of the signal

Equations 3.1.1 to 3.1.8 show the complete set of calculations involved in computing *TDL*.

Some say it is not possible to accurately model the diffraction losses that occur from terrain. For this reason many researchers choose to omit diffraction effects from their studies, eliminating all shadowed areas from their results (Schwering et al. 1988; Dal Bello et al. 2000). Deygout defends his diffraction methodology as sound in his 1991 paper. Based on applying his own algorithms for 21 years, he asserts that the mean error of his cumulative data collection is 1 dB, with a standard deviation of 4-5 dB. He speculates that the errors people tend to have with his methodology are largely due to inaccurate terrain models. He notices that the greatest errors tend to occur with the greatest transmitter-receiver separation. Since his methodology is iterative, each error in the elevation of an obstruction compounds, generating gross errors at far distances.

CHAPTER IV

AVAILABLE DATA

Cell Phone Tower Data Set

A confidential cell phone tower data set was obtained for one Provider for the state of North Carolina. All locations are for digital towers, which fall in the 1850 to 1990 MHz range. The towers are divided into sectors, with three per tower in most cases. The data set consists of latitude and longitude in the datum World Geographic System (WGS) 1984, antenna heights and sector azimuths. Most antennas for Provider have three sectors with azimuths 120 degrees apart. By having three sectors, the antenna achieves coverage approximating the shape of a circle. The azimuth is measured in degrees from north. Figure 4.1 shows a typical antenna propagation pattern with sector azimuths 120 degrees apart.

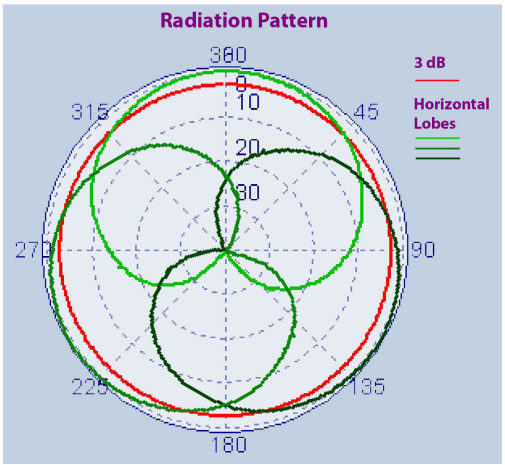

Figure 4.1. Three Sector Antenna Propagation Pattern

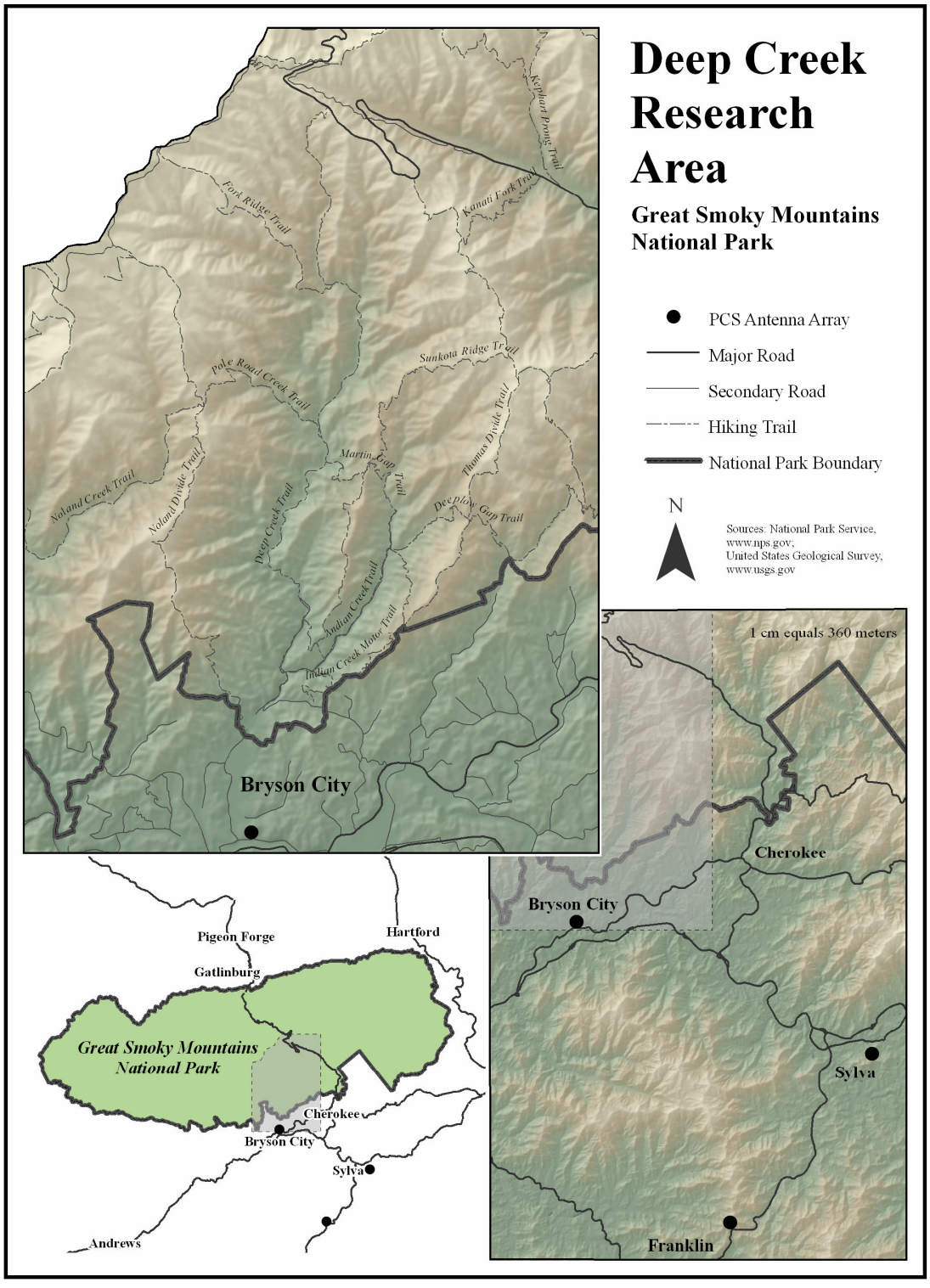

Figure 4.2. Geographic Research Area

An area of interest was chosen just north of Bryson City, North Carolina. The park refers to this area as Deep Creek. Three Provider towers impact this area, with their locations shown in Figure 4.2. The towers vary in height and elevation, while each supports three sectors at azimuths 0, 120 and 240.

LIDAR Data Set

An all returns LIDAR data set for the area of interest was obtained from the North Carolina Floodplain Mapping Program. This LIDAR was flown at the beginning of 2005 in leaf off season to facilitate the acquisition of bare earth data, particularly in forested areas (NCFM, 2006). Earthdata International performed a proprietary filtering of the data points. An independent accuracy assessment found that the DEMs generated from the filtered LIDAR points located in the park had an RMSE of 1.42 ft (0.43 m), with the standard deviation of the vertical errors being 1.44 ft (0.44 m) (NCFM 2006).

Vegetation Classification Data Set

A classified map of the Great Smoky Mountains National Park was obtained from the National Park Service (NPS). The NPS Vegetation Map is comprised of forty classes. Each class is a combination of over- and undercanopy types. The NPS began its vegetation mapping in the Cades Cove and Mount Le Conte quads because they believe the vegetation contained in these regions to be representative of the diversity of the park (ESRI 2000). The classification was supervised, involving the advance collection of field observations prior to photointerpretation (The Nature Conservancy 1999). The remainder

of the park was classified by comparing a variety of aerial imagery to the classes in the pilot quads. The park finished its accuracy assessment at the beginning of 2007. They estimate the overall accuracy of the map to be 80%. The assessment points collected within the area of interest had a lower accuracy of 78% (Jenkins 2007).

CHAPTER V

METHODOLOGY

Field Data Collection

Field measurements were conducted along the trails of the Deep Creek region, located north of Bryson City and south of Clingman's Dome. It was determined that three towers could be impacting this area based on their distances and elevations. As this research is interested in visualizing the reception hikers can expect in the park, data collection was conducted along the roads and trails. A stratified random sample of trail segments was selected representing approximately 20% of the trails within the area of interest. Using a 10-meter DEM acquired from the USGS, a preliminary viewshed showed which trails had areas within the line of sight and which trails were completely outside the line of sight. Half the sample was taken from each of these categories in order to ensure that measurements would include trails within the line of sight for post processing.

The FCC Universal Licensing System was consulted to determine the frequency bands reserved by Provider in the geographic area of interest. Two band widths were reserved in the area, 1870-1885 MHz and 1950-1965 MHz. A spectrum analyzer survey of the three antenna sites concluded that each of these antennas was operating within the 1950-1965 MHz band.

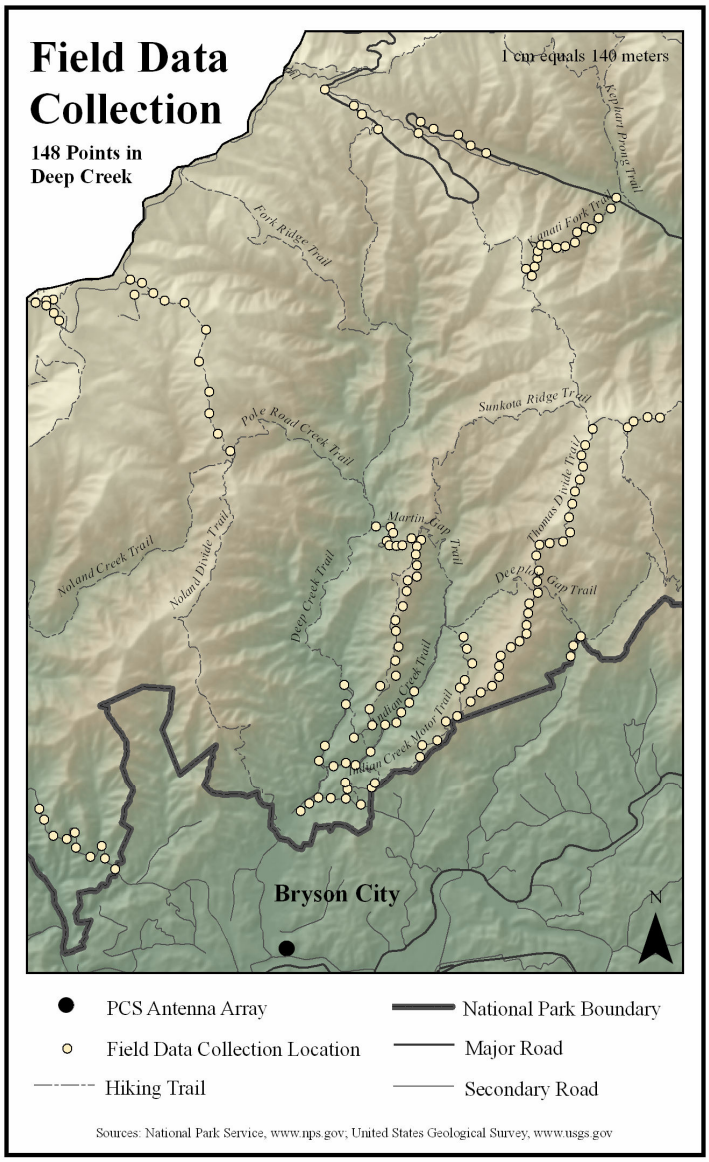

Figure 5.1. Field Data Collection Locations

Along each randomly selected road or trail, measurements were taken at equal intervals, approximately 300 meters apart. A total of 148 points were visited. At each point the following data were collected: GPS coordinates, and received signal power. At 73 of the 148 locations, the approximate tree canopy height was also measured. The GPS device had a horizontal accuracy of one meter and an estimated vertical accuracy of two meters. The tree canopy heights were calculated using a clinometer to measure the height of a typical tree in the area. The accuracy of this methodology is approximately 4 meters. The received signal level measurement had an accuracy of 3 percent according to equipment specifications. Figure 5.1 shows the locations of each data collection point.

Elevation Model Creation

The all returns LIDAR data from the North Carolina Floodplain Mapping Program was divided into two data sets – last returns and first returns. All points with the same geographic coordinates were separated between the maximum elevation and the minimum elevation. The data was then evaluated for outliers. Typical outliers are first returns that capture birds, clouds, or any other elevation that is above the ground canopy (Hyde et al. 2007). Any point greater than 100 meters above or below others in the geographic vicinity was eliminated by a visual survey.

The minimum elevation does not necessarily represent the ground level, as tree crowns may stop the signal entirely before it hits the ground. With this situation in mind, the minimum elevation values were further filtered according to the methodology devised by Kobler et al. (2007). Six independent random samples with replacement were taken

from the last returns dataset, each representing 23% of the entire dataset. The resulting six sample datasets had an average of 145 points per hectare. According to Anderson et al., at least 143 points per hectare can be used to create a 5-meter DEM (2006). They determined that a smaller cell size would result in unnecessary computer processing time with no additional accuracy. Each of the six samples was interpolated to a 5-meter DEM using the inverse distance weighting algorithm.

These grids were processed to obtain a local minimum for each grid cell in the area of interest. The output grid containing the local minimums was then used along with the six sample grids to calculate the *gmo*. The local *gmo* for each cell is represented by the average differences across all six grids (Equation 5.1).

$$d_{ij} = z_{ij} - z_{j,min} \qquad (5.1)$$

Where z_{ij} is the i-th elevation estimate at the j-th location
and $z_{j,min}$ is the lowest elevation estimate at the j-th location.

The *gmo* for the entire dataset is the average of all the local *gmo*'s. The *gmo* for the area of interest was calculated to be 1.83 meters. The *gmo* was added to each cell in the minimum elevation grid to produce the final REIN elevation grid.

This methodology was repeated with the first returns, to create five sample grids. The maximum, instead of the minimum, was calculated at each grid cell location. Similarly the *gmo* (2.7 m) was subtracted from the maximum elevation grid to produce a final canopy grid. Kobler et al. did not test the REIN algorithm as a methodology for creating a tree canopy model (2007). Therefore an error analysis will be key in determining the usefulness of the canopy grid.

Predicted Signal Strength Calculations

In order to obtain a predicted signal strength for each field collected point, the first step was to calculate the free space loss. If the transmitted power level of the antenna is known, the Friis free space formula (Equation 2.1) can be used to approximate the amount of power remaining in the radio wave when it reaches the receiver. Unfortunately Provider did not respond to inquiries related to the power level of their antenna systems. Therefore additional field work was conducted to create a reference point from which additional free space calculations could be derived. If the researcher has a known power level at a known distance from the antenna, additional power values can be calculated relative to that reference power level (Molish 2005, Rappaport 2002). Equation 5.2 shows that the measured power from a reference distance $P_r(d_0)$ can be used to predict the signal power at another distance from the antenna.

$$P_r(d) = P_r(d_0)\left(\frac{d_0}{d}\right)^2 \qquad d \geq d_0 \geq d_f \qquad (5.2)$$

P_r = receiver power in milliwatts
d = transmitter-receiver separation in meters
d_0 = received power reference point

where $d_f = 2D^2 / \lambda$
and D = largest physical linear dimension in meters
on the transmitter antenna

Tables 5.1 and 5.2 show the results of the measurements taken to calculate the reference power of each transmitter. An average was taken of the measurements around each tower and used in Equation 5.2 as d_0. Using this value combined with the actual distance

Table 5.1. Measurements for Reference Power Calculation

Tower	Received Signal Levels (dBm) at 1 km
Bryson City	-50.4
	-58.4
	-61.2
	-60.0
	-76.8
	-68.4
Sylva	-70.8
	-81.6
	-61.2
	-69.2
	-79.2
	-87.2
	-66.0
	-73.2
	-75.2
	-67.2
	-63.6
	-71.2
Franklin	-67.2
	-70.4

Table 5.2. Reference Power Values

Tower	Average Power in dBm at 1 km	Average Power in mW at 1 km
Bryson City	-62.5	5.62×10^{-7}
Sylva	-73.1	4.90×10^{-8}
Franklin	-68.8	1.32×10^{-7}

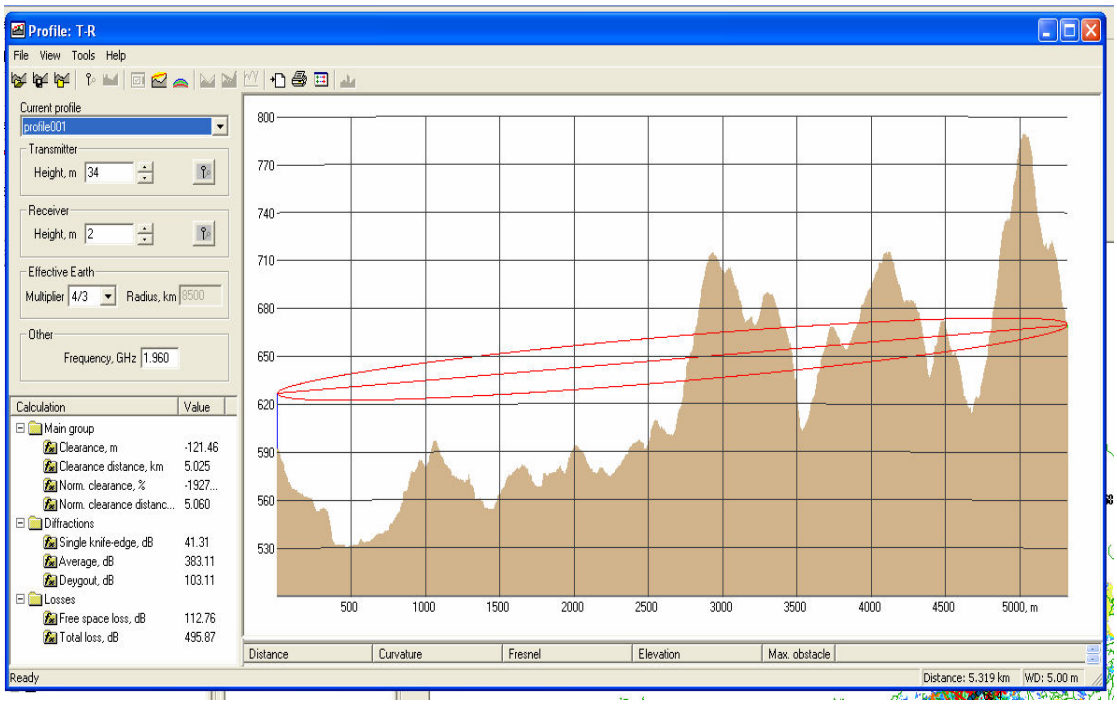

Figure 5.2. Sample Profile Between Transmitter and Receiver

separations, $P_r(d)$ was evaluated for each point from the perspective of each tower, resulting in three predictions at each site.

The output ground elevation DEM from the LIDAR analysis was then input into Cellular Expert along with the locations and heights of the towers of interest. A profile was created between each tower and each data point (see Figure 5.2). Each profile shows how far the radio wave would travel and the location and height of each terrain obstacle. Most importantly, the profile also calculates the Deygout diffraction for each path. The Deygout diffraction value was added to the free-space value, resulting in a loss prediction including terrain as a variable.

Three predictions were available for each data collection point, accounting for the independent variables of frequency, distance and terrain. The received signal level measurements collected in the field represented the strongest signal available within that bandwidth at that location. Therefore the highest of each of the three predicted values was gleaned from the calculations for comparison to the field collected data. Differences between observed and measured values were analyzed, with the hopes that the residuals could be attributed to land cover attributes.

CHAPTER VI

ANALYSIS AND RESULTS

Accuracy Assessments

GPS Terrain Heights

The REIN terrain elevation grid was assessed for accuracy based on the GPS collected points from the field data collection. The average absolute error between the GPS readings and the REIN grid was 4.17 meters, and the standard deviation 4.44 meters. A histogram of the elevation errors is shown in Figure 6.1. The skewness is -0.391, indicating that the mass of the distribution is concentrated on the right side of the histogram. This would indicate that more often than not, the observed value was greater than the value predicted by the REIN grid. An average absolute error of 4.17 meters is greater than expected considering the 0.43 m accuracy asserted by the North Carolina Floodplain Mapping Program. However the observed values being more often greater than predicted values could indicate that the REIN algorithm did what it claimed, in that it eliminated the impact of tree crowns from the final DEM.

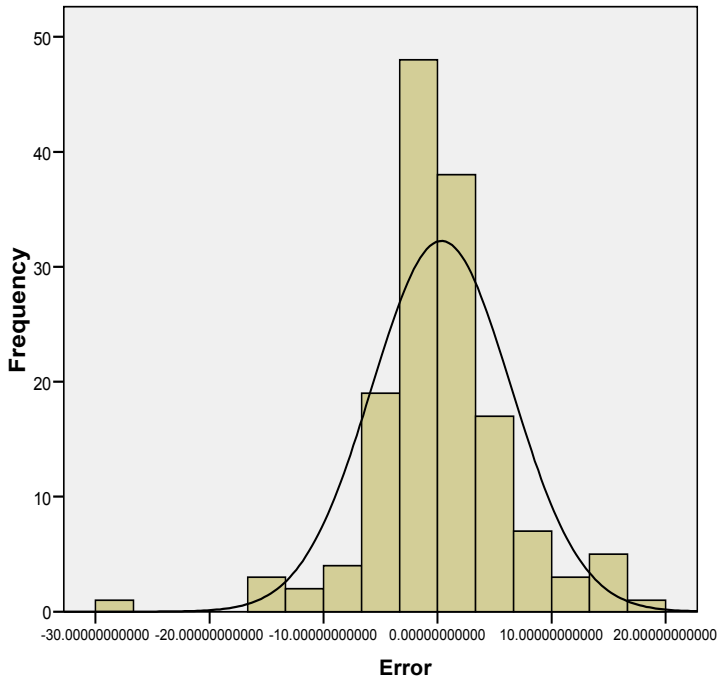

Figure 6.1. Histogram of Elevation Errors (Observed Minus Predicted)

Over-Canopy Grid

Next the REIN canopy elevation grid was assessed for accuracy based on the clinometer calculations of an average tree at 73 GPS collected points. The average absolute error between the clinometer readings and the REIN grid was 10.08 meters, and the standard deviation 6.55 meters. A histogram of the elevation errors is shown in Figure 6.1. The skewness is -0.141, indicating that the mass of the distribution is slightly concentrated on the right side of the histogram. This would indicate that more often than not, the observed value was greater than the value predicted by the REIN grid. Only 7 points were over-estimated by the model, while 93 points were underestimated by the model. Therefore for 89% of all the points, the canopy grid gave a value lower than the

ground truth. This would indicate that despite the density of the trees in this area, LIDAR points collected in leaf off conditions are not sufficient for creating a canopy grid using the REIN algorithm.

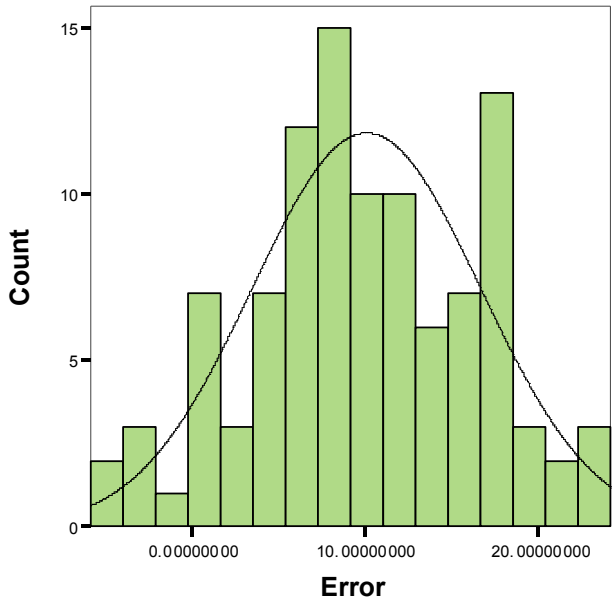

Figure 6.2. Histogram of Canopy Height Errors (Observed Minus Predicted)

Signal Strength Calculations

The noise floor published in the specifications of the spectrum analyzer is -110 dBm. As the signal approaches -110 dBm, the likelihood increases that the any reading would only reflect environmental noise or noise internal to the unit. Close to -108 dBm, the cell phone tower signal becomes indiscernible from that noise. Therefore any signal strength that was recorded as less than -108 dBm is suspect. In such a case the truth could be -108 dBm, or the truth could be lower. It would be impossible to tell with this set of equipment. In order to avoid this type of suspect data, all observations less than

-108 dBm were removed from all signal strength analyses. The remaining dataset consisted of 103 points.

For each data point there was a leaf on and leaf off reading. These observations were compared to the computer model which was calculated based on the Friis and Deygout equations. As discussed earlier, Cellular Expert, and extension of ESRI's ArcMap, aided in the complex Deygout calculations. Signal strength calculations involving terrain were based on the REIN final terrain map.

Seven observations were calculated to be within the direct line of sight of the tower contributing the strongest signal at that location. Figure 6.3 shows how the leaf-on and leaf-off observations compare to the Friis free space model.

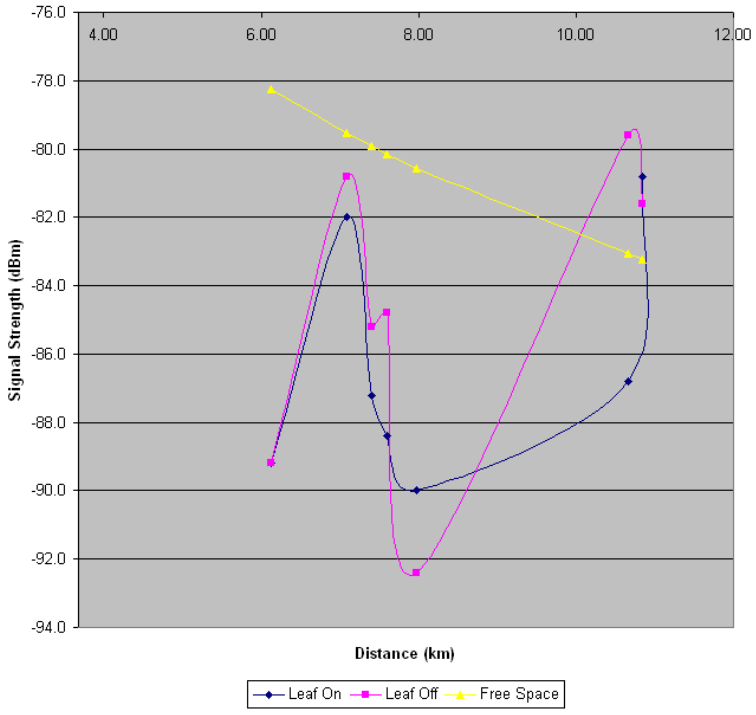

Figure 6.3. Line of Sight Signal Strength Readings Compared to Free Space Model

In five of the seven cases, the measured value was less than the free space value. This follows the hypothesis that field collected measurements within dense vegetation would be lower than a free space calculation. It is interesting to note that the two last anomalous points are both much farther from their antenna than the other five.

Figure 6.4 shows how closely the field measurements came to the ideal predicted value for all 103 cases. It shows that as the predicted signal strength decreases, the gap between the model and the reality increases. The mean leaf-on error was -37.6, while the mean leaf-off error was -40.3. The standard deviations were similar, 27.5 and 28.6

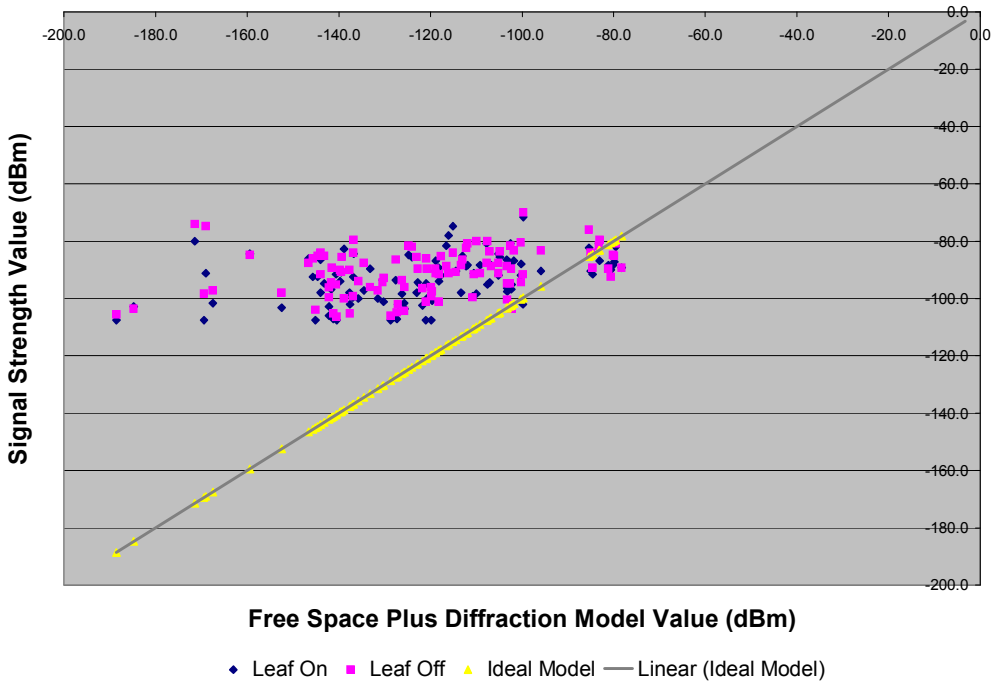

Figure 6.4. Ideal Free Space Plus Diffraction Model Compared to Observed Values

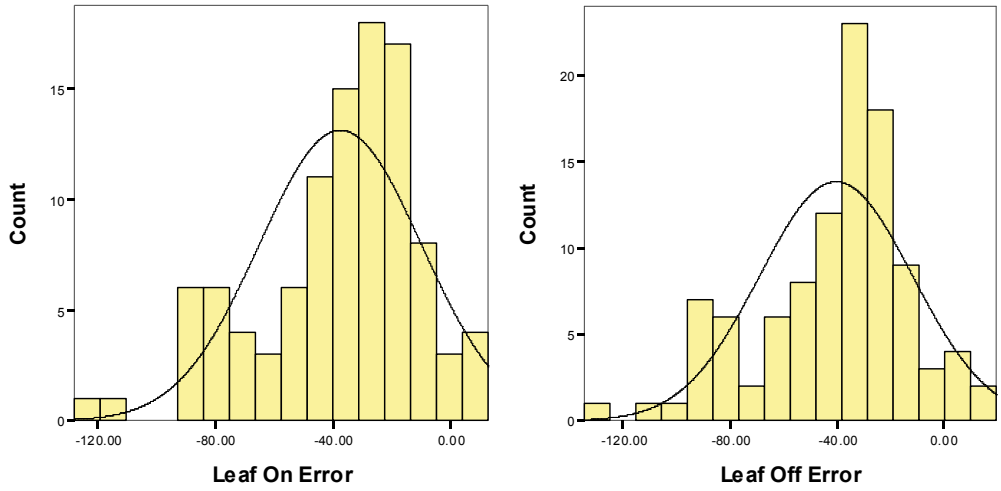

Figure 6.5. Ideal Free Space Plus Diffraction Model Error, Leaf On and Leaf Off

respectively. Both have a -0.7 skewness, showing once again that the observed values tended to be greater than the predicted values (See Figure 6.5).

The ideal model compared well in cases where diffraction around ridges was not a factor. However the ideal model did not do nearly as well in the other 96 cases where Deygout diffraction was calculated. Since the elevation model had an average error of about 4 meters, it is probable that the prediction accuracy was strongly impacted by the quality of the REIN grid. This problem, documented by Deygout and his critics has created an experimental obstacle here as well (Deygout 1991). The proposed methodology was to compute free space and diffraction for each point, then to assume that the difference between that computation and reality was solely due to other variables. Without conducting much more extensive field measurements, it is impossible to know the exact elevation of each ridge which lies between each point and its antenna. The

relative inaccuracy of the terrain model now renders this approach impossible since the data are not available at this time to have an accurate Deygout calculation for each point.

Vegetation Classification

In classifying the Great Smoky Mountains National Park, the National Park Service used the Community Element Global Codes (CEGL) from the National Vegetation Classification Standard. Since the vegetation of this area is among the most diverse in the world, the ecologists found that certain CEGL classes were prone to be misconstrued. Although they observed 58 distinct CEGL classes, they chose to combine several classes that were indistinguishable in the remotely sensed data. The result was 40 distinct classes, 31 of which are CEGL classes, and the remaining 9 of which fell outside this classification system (ex. roads, rock, gravel, etc.).

For the current data analysis, the remaining 31 CEGL classes were consolidated into four distinct categories: evergreen, northern hardwood, oak-hickory, and cove hardwood. The polygons which fell outside the classification system were invariably small. For the sake of analysis, the closest class within the NPS system was observed and applied. Table 6.1 shows how the NPS classes contained in the AOI were consolidated to become four analysis classes.

Of the 103 points remaining in the sample, 11 were evergreen, 18 were northern hardwood, 69 were oak-hickory, and 6 were cove hardwood. Table 6.2 shows the distribution of the points compared to the actual distribution of the vegetation classes within the area of interest. In this table the population statistics include the entire area of interest, whereas the data collection points were limited by trail access.

Table 6.1. Consolidation of Analysis Categories

Analysis Categories	NPS Code
Evergreen 250 – 2000m elevation, mesic soil *Includes formerly mixed spruce-fir forests, where some or nearly all the firs have been killed by the balsam wooly adelgid. Evergreen areas with pine also include various kinds of oak and hickory.*	1013 – spruce-fir 1001 – yellow pines 7517 – eastern white pine
Northern Hardwood 1000 – 1500m elevation, mesic soil *Traditionally birch, beech and buckeyes. Birch is most prolific, but also has spruce, hemlock and red maple.*	6124 – forested boulderfield 1010 – northern and acid hardwoods 1011 – northern hardwoods and boulderfields
Oak-Hickory 250 – 1500m elevation, sub-mesic soil *Various kinds of oak and hickory, with some birch and red maple.*	6192 – oak hardwood with red maple 7230 – oak hardwood with hickory 7692 – oak hardwood rich type 1007 – chestnut oak 1008 – high elevation beech and red oak 1009 – high elevation red and white oak
Cove Hardwood 250 – 1000m elevation, mesic soil *Maple, tuliptree and birch abound. Hemlock is fairly common.*	7543 – cove hardwood acid type 7710 – cove hardwood typic 1003 – floodplain forest 1006 – successional hardwood

Table 6.2. Distribution of Sample by Vegetation Analysis Class

Analysis Category	Sample Frequency (# of points)	Sample Percent	Population Frequency (ha)	Population Percent
Evergreen	11	10.6	2,352	10.1
Northern Hardwood	18	17.3	6,238	26.7
Oak-Hickory	69	66.3	9,828	42.1
Cove Hardwood	6	5.8	4,947	21.2
TOTAL	104	100	23,365	100

For each of its vegetation classes, the park has an inferred soil moisture category (Madden 2004). Those categories were recorded for each NPS code and related to each data collection point. They describe the overall moisture trends of that particular vegetation class across time. The high moisture category gets plenty of precipitation in prime growth times. The low moisture category gets much less precipitation, and the little it gets is in the winter.

Statistical Analysis

The differences between observed and predicted signal strength values proved to be great, and could probably be attributed to the quality of the terrain modeling. Although it may not be possible at this time to attribute all the residuals to land cover variables, it is still useful to look at how the environmental attributes could have contributed in part to the signal strength measurements. To that end, three sets of comparisons were run. Each one assessed the contributions that the land cover variables made to leaf on measurements, leaf off measurements and the difference between local leaf on and leaf off measurements. Independent variables included vegetation type, soil moisture content, measured tree canopy height, and distance from the dominant antenna.

ANOVA Tests

ANOVA tests were run to test the impact of the independent variables of vegetation type and soil moisture content on the signal strength measurements. The soil moisture levels reported by the NPS were nominal, distinguishing between dry, wet and medium soil types. As seen in Table 6.3, the only significant result seen in these ANOVAs is the impact of soil moisture on the difference between leaf on and leaf off measurements. Figure 6.6 shows the differences in means graphically. While the medium and low moisture categories had similar means, the high moisture category was significantly different.

There was no significant difference in means between the four vegetation categories and the difference between the leaf on and leaf off measurements. The ANOVA results for this test are shown in Figure 6.7.

Table 6.3. ANOVA Test Results With Signal Strength as the Dependent Variable

Dependent Variables	Independent Variables			
	Vegetation Type		Soil Moisture	
	F-Value	P-Value	F-Value	P-Value
Leaf On Signal Strength	0.66	0.5790	0.24	0.7860
Leaf Off Signal Strength	2.58	0.0582	2.30	0.1054
Leaf Off – Leaf On	2.09	0.1061	5.83	0.0041*

* p-value is significant ($\alpha = 0.05$)

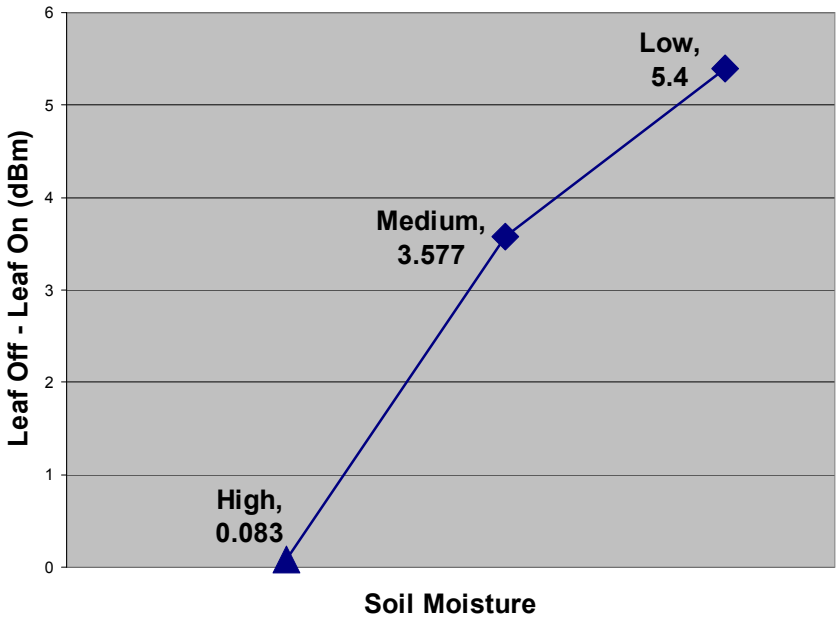

Figure 6.6. Soil Moisture as the Main Effect for the Difference Between Leaf Off and Leaf On Measurements. The different symbols indicate a significant difference between each category.

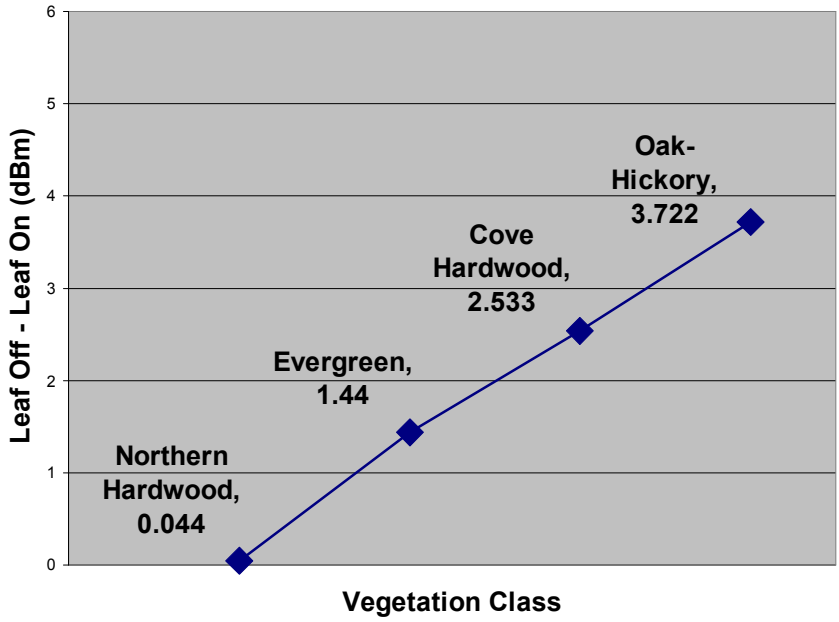

Figure 6.7. Vegetation Class as the Main Effect for the Difference Between Leaf Off and Leaf On Measurements.

In order to test the possibility of the independent variables being correlated in some way, ANOVAs were also run testing the impact of vegetation type and soil moisture content on tree canopy height and distance from the dominant antenna. The results are shown in Table 6.4. Significant differences in means were found in all cases. Tree canopy height varies by vegetation type and by soil moisture, while distance also varies by vegetation type and soil moisture. Figures 6.8 and 6.9 graphically show the difference in means of the tree canopy heights, with vegetation type and soil moisture respectively as the main effects.

Table 6.4. ANOVA Test Results With Tree Canopy Height and Distance from Dominant Antenna as the Dependent Variables

Dependent Variables	Independent Variables			
	Vegetation Type		Soil Moisture	
	F-Value	P-Value	F-Value	P-Value
Tree Canopy Height	6.00	0.0040*	7.46	0.0080*
Distance from Dominant Antenna	8.12	<0.0001*	11.32	<0.0001*

* p-value is significant ($\alpha = 0.05$)

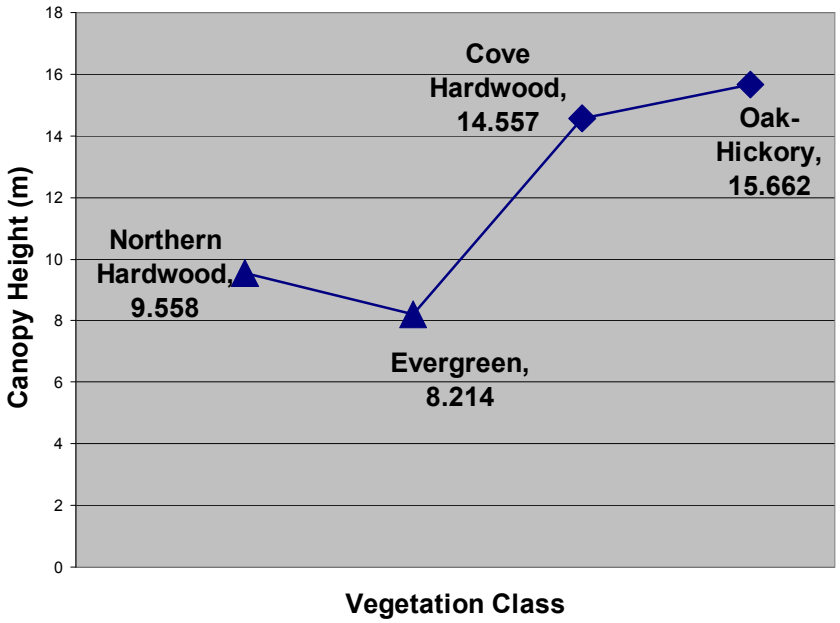

Figure 6.8. Four Vegetation Classes as the Main Effect for the Measured Canopy Height. The different symbols indicate a significant difference between each category.

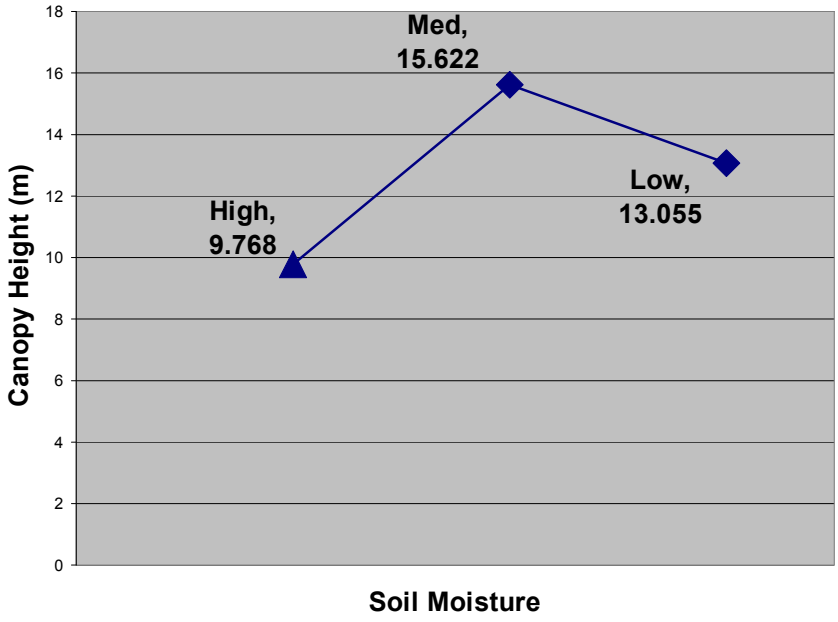

Figure 6.9. Soil Moisture as the Main Effect for the Measured Canopy Height. The different symbols indicate a significant difference between each category.

Correlation Tests

Since the independent variables of tree canopy height and distance are interval/ratio data types, it was possible to use a correlation to test their relationship to signal strength. Table 6.5 shows that a significant negative correlation exists between leaf off signal strength and distance. Tree canopy height has a positive correlation to the leaf on leaf off difference, however distance has a negative correlation to the leaf on leaf off difference. For every meter the tree canopy increases, the signal strength gap increases by 0.283 dBm. Conversely, for every meter the transmitter-receiver distance increases, the signal strength gap decreases by 0.290 dBm.

Table 6.5. Correlation Test Results With Signal Strength as the Dependent Variable

Dependent Variables	Independent Variables			
	Tree Canopy Height		Distance	
	R-Value	P-Value	R-Value	P-Value
Leaf On Signal Strength	-0.108	0.3638	-0.085	0.3915
Leaf Off Signal Strength	0.106	0.3710	-0.298	0.0022*
Leaf Off – Leaf On	0.283	0.0154*	-0.290	0.0030*

* p-value is significant ($\alpha = 0.05$)

The possibility of a correlation between distance and tree canopy height was investigated. The r-value was -0.210, indicating a potential negative correlation. However the p-value was 0.0742, which is not small enough to indicate a significant relationship between the two variables.

Discussion of the Results

There were few significant findings relating the independent variables directly to the field measured values. None of the independent variables significantly impacted the leaf on measurements. Distance was found to be the only significant predictor of leaf off measurements, with a p-value of 0.0022. Not surprisingly, the closer the receiver, the higher the signal strength. In light of that finding, it is interesting to note that distance was *not* a significant predictor of leaf on signal strength. This lack of significance actually bolsters the hypothesis that leafy vegetation does indeed play an independent role on signal attenuation.

An analysis of the differences between the seasonal values at each data collection point reaped the most interesting results. There was no significant difference in means between the four vegetation categories. Figure 6.7 shows that although at face value the four classes appear to be different, the p-value for the ANOVA was 0.1061.

If the vegetation categories were to be consolidated into two classes, a different story would emerge. Figure 6.10 shows that there is a significant difference in means between the two categories of Northern Hardwood and Evergreen, and Oak-Hickory and Cove Hardwood.

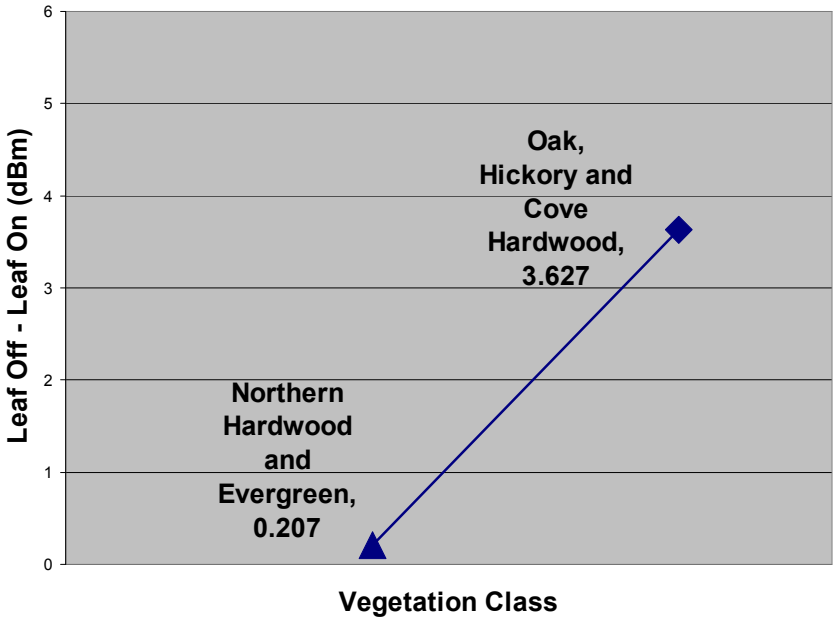

Figure 6.10. Vegetation Class as the Main Effect for the Difference Between Leaf On and Leaf Off Measurements. The different symbols indicate a significant difference between each category.

The first category is dominated by spruce, fir, pine, beech, birch and red maple. The second category is dominated by various types of oak (red, white and chestnut), tulip poplar, and hickory. These categories might seem arbitrary, but they are actually connected to other environmental characteristics. The first category has an average

canopy height of 9 meters, while the second has an average canopy height of 15 meters. The ANOVA showing the effect of the vegetation category on canopy height shows that Northern Hardwood and Evergreen as a group have significantly different canopy heights than Oak-Hickory and Cove Hardwood (Figure 6.8). This trend implies that canopy height by itself could tell more of the story than tree species.

A correlation comparing the measured canopy height to the seasonal differences showed a significant positive correlation of 0.28, with a p-value of 0.0154. The higher the canopy, the more the signal improved in the winter. For every meter increase in the canopy, the signal improved by 0.28 dBm when the leaves fell.

Distance was also found to be a predictor of the magnitude of the change between leaf on and leaf off. A negative correlation of -0.29 was found between the two, with a p-value of 0.003. For every meter increase in distance between the antenna and the receiver, the gap between leaf on and leaf off diminished by 0.29 dBm. Since there was no significant correlation between canopy height and distance, distance could be having its own unique impact on the signal. The farther the distance, the less the leafy vegetation impacts further attenuation.

Finally, soil moisture was found to have a significant impact on the leaf on v. leaf off difference. It was also shown to be linked to tree canopy height and distance. It is unlikely that distance from the antenna is plays a direct role in the composition of the soil, or in the signal strength differences. In all the studies that have looked at distance as a variable, one was not found that correlated short distances with the potential for high clutter interference. It is possible that a causal connection exists between soil moisture

and tree height. How the soil moisture and canopy height combine to predict signal strength loss is not entirely clear. The higher the moisture content, the less the signal strength gap. The higher the canopy, the more the signal strength gap. The higher the soil moisture, the lower the canopy. The results seem counterintuitive. They may have been impacted by the number of observations in each class. Whereas high and medium moisture contain 29 and 71 points respectively, low only holds 4 sample points. Soil moisture could also easily be a barometer for another environmental variable not considered here.

CHAPTER VII

CONCLUSION

Up to this point radio propagation research involving vegetation has focused on determining differing loss values for different tree species. This study has uncovered a significant new angle of research, indicating a need to focus on other environmental attributes. Significant relationships were found relating soil moisture and tree heights to attenuation. According to the data collected, the height of the tree canopy was a more significant contributor to attenuation than the species of the tree. In fact, the vegetation classes were not found to be indicators at all until they were grouped according to mean heights. In this study the species of tree was only significant insomuch as it was an indicator of the tree height.

In light of this discovery it was disappointing that the tree canopy grid proved to be inadequate for modeling. Leaf on LIDAR data would certainly yield a much better digital model, however this data is harder to find and often has not been collected. An alternative to creating a model through LIDAR would be to use generalized tree height data regularly collected by the National Park Service and other entities. Each vegetation category could be given an approximate canopy height to input into a path loss calculation.

The soil moisture variable deserves further consideration in future studies. It is unlikely that the soil in an of itself is impacting signal loss. It is much more plausible

that the soil moisture content is impacting other aspects of the physical environment. This study did not differentiate between successional and old growth forests. Successional forests are going through a process of regrowth. They can have plenty of annual precipitation but a low canopy of young tree stands. If a correlation were found between successional forests and high soil moisture, that might account for the finding that moisture impacts signal attenuation. It is also possible that the undercanopy is playing a role, as bushes were often taller than the height of the field data collection equipment. The makeup of the undercanopy can also vary according to the precipitation. Ideally further studies would include a greater volume of points within the line of sight of the antenna. Removing the variable of terrain diffraction could help clarify some of these questions.

Finally, in the interests of creating excellent propagation maps without the need for expensive field data collection, greater attempts should be made to improve the accuracy of elevation modeling in this context. Different algorithms for LIDAR filtering could yield improved diffraction calculations. There is value in comparing the performance of various LIDAR filtering and terrain modeling techniques.

Every improvement of wireless modeling in rural settings is a step toward a better understanding of how radio waves interact with the environment. Improved understanding creates better management of resources and minimization of the visual impact of towers. As urbanization continues to eliminate green spaces in the United States, the popularity of park recreation will only increase. Concerns over safety have always been and will continue to be an issue in the future. Rural areas experience the

same public health and emergency concerns as urban areas. Popular recreation spots with regular incidents and poor coverage are particularly disadvantaged in the face of a crisis.

Predicting cell phone coverage for wilderness areas frequented by novice hikers makes good sense. The National Park Service has grown in the last hundred years from a few hundred thousand visits to 275 million visits each year (NPS 2007). Incidents will happen. An understanding of how to predict and visualize wireless coverage in parks will be an asset for the future.

REFERENCES

Anderson, Eric S., James A. Thompson, David A. Crouse, Rob E. Austin. 2006. Horizontal resolution and data density effects on remotely sensed LIDAR-based DEM. *Geoderma* 132: 406-415.

Bullington, K. 1947. Radio propagation at frequencies above 30 megacycles. *Proceedings of the Institute of Radio Engineers* 35: 1122-1136.

CTIA. 2007. *CTIA's Semi-Annual Wireless Industry Survey Results.* http://files.ctia.org/pdf/CTIA_Survey_Mid_Year_2007.pdf (accessed March 18, 2008).

Copeland, Larry. 2007. More hikers wind up lost. *USA Today*. September 3.

Dal Bello, Julio Cesar R., Glaucio L. Siqueira, Henry L. Bertoni. 2000. Theoretical analysis and measurement results of vegetation effects on path loss for mobile cellular communications systems. *IEEE Transactions on Vehicular Technology* 49, no. 4: 1285-1293.

Deygout, J. 1966. Multiple knife-edge diffraction of microwaves. *IEEE Transactions on Antennas and Propagation* 14, no. 4: 480-489.

-------. 1991. Correction factor for multiple knife-edge diffraction. *IEEE Transactions on Antennas and Propagation* 39, no. 8: 1256-1258.

Environmental Systems Research Institute. 2000. *Photo Interpretation Report USGS-NPS Vegetation Inventory and Mapping Program Great Smoky Mountains National Park Cades Cove and Mount Le Conte Topographic Quadrangles Pilot Sudy*

Area. http://biology.usgs.gov/npsveg/ftp/vegmapping/grsm/reports/ grsmrpt.pdf (accessed March 9, 2007).

Epstein, J., and D. W. Peterson. 1953. An experimental study of wave propagation at 850 Mc. *Proceedings of the International Radio Engineers* 41: 595-611.

Federal Communications Commission. 2000. *OET Bulletin No. 71 - Guidelines for testing and verifying the accuracy of wireless E911 location systems*. http://www.fcc.gov/911/enhanced/ (accessed March 9, 2007)

-------. *FCC amended report to congress on the deployment of E-911 phase ii services by Tier III service providers*. http://hraunfoss.fcc.gov/edocs_public/attachmatch/ DOC-257964A1.pdf (accessed March 9, 2007).

Fraser, Thomas. 2002. Park near having first fatality-free year since 1971. *Maryville Daily Times*. December 22.

Goldman, J. and G. W. Swenson, Jr. 1999. Radio wave propagation through woods. *IEEE Antennas and Propagation Magazine* 41, no. 5: 34-36.

Hata, Masaharu. 1980. Empirical Formula for Propagation Loss in Land Mobile Radio Services. *IEEE Transactions on Vehicular Technology* 29, no. 3: 317-325.

Hernando, Josae M., and F. Paerez-Fontaan. 1999. *Mobile Communications Systems*. Boston: Artech House, Inc.

Hyde, Peter, R. Dubayah, B. Peterson, J. B. Blair, M. Hofton, C. Hunsaker, R. Knox, and W. Walker. 2005. Mapping forest structure for wildlife habitat analysis using waveform LIDAR: Validation of montane ecosystems. *Remote Sensing of Environment* 96, no. 3: 427-437.

Jacobsen, K. and P. Lohmann. 2003. Segmented filtering of laser scanner DSMS. http://www.isprs.org/commission3/wg3/workshop_laserscanning/papers/Jacobsen_ALSDD2003.pdf (accessed April 25, 2007).

Jenkins, Michael. 2007. *Thematic Accuracy Assessment: Great Smoky Mountains National Park Vegetation Map*. Gatlinburg: National Park Service, Great Smoky Mountains National Park.

Kilian, J., N. Haala, and M. Englich. 1996. Capture and evaluation of airborne laser scanner data. In *International Archives of Photogrammetry and Remote Sensing, Vol. XXXI,* 383-388. Vienna: ISPRS Congress**.**

Kobler, Andrej, Norber Pfeifer, Peter Ogrinc, Ljupco Todorovski, Kristof Ostir, and Saso Dzeroski. 2007. Repetitive interpolation: a robust algorithm for DTM generation from aerial laser scanned data in forested terrain. *Remote Sensing of Environment* 108, no. 1: 9-23.

Kraus, K, and N. Pfeifer. 1998. Determination of terrain models in wooded areas with airborne laser scanner data. *ISPRS Journal of Photogrammetry and Remote Sensing* 53: 193-203.

Madden, Marguerite, Roy Welch, Thomas Jordan and Phyllis Jackson. 2004. Digital Vegetation Maps for the Great Smoky Mountains National Park. Athens, GA: Department of Geography at the University of Georgia.

Molisch, Andreas F. 2005. *Wireless Communications*. West Sussex: IEEE Press.

National Park Service. 2007. *Transportation in the Parks*. http://www.nps.gov/transportation/ (accessed March 9, 2007).

Nature Conservancy, The. 1999. *USGS-NPS Vegetation Mapping Program: Vegetation Classification of Great Smoky Mountains National Park (Cades Cove and Mount Le Conte Quadrangles)*. http://biology.usgs.gov/npsveg/ grsm/methods.pdf (accessed March 9, 2007).

North Carolina Floodplain Mapping Program. 2003. *LIDAR and Digital Elevation Data*. http://www.ncfloodmaps.com/pubdocs/ lidar_final_jan03.pdf (accessed March 9, 2007).

-------. 2003. *Summary of the Program Fact Sheet*. http://www.ncfloodmaps.com/ pubdocs/ncstatusdocument_jan03-4pager.pdf (accessed April 23, 2007).

-------. 2006. *LIDAR Accuracy Assessment Report: Swain County*. http://www.ncgs.state.nc.us/flood/qc_reports/Lidar_QA_Swain.pdf (accessed February 27, 2008)

Ott, R Lyman, and Michael Longnecker. 2001. *An Introduction to Statistical Methods and Data Analysis*. Pacific Grove: Thomas Learning, Inc.

Rappaport, Theodore S. 2002. *Wireless Communications: Principles and Practice*. Upper Saddle River: Prentice-Hall, Inc..

Roberts, Scott D., Thomas J. Dean, David L. Evans, John W. McCombs, Richard L. Harrington, and Patrick A. Glass. 2005. Estimating individual tree leaf area in loblolly pine plantations using LIDAR-derived measurements of height and crown dimensions. *Forest Ecology and Management* 213: 54-70.

Rogers, N. C., A. Seville, J. Richter, D. Ndzi, N. Savage, and R. F. S. Caldeirinha. 2002. *A Generic Model of 1-60 GHz Radio Propagation through Vegetation - Final*

Report. http://www.ofcom.org.uk/static/archive/ra/topics/research/topics/propagation/vegetation/vegetation-finalreportv1_0.pdf (accessed March 7, 2007).

Rubinstien, Thomas N. 1998. Clutter losses and environmental noise characteristics associated with various LULC categories. *IEEE Transactions on Broadcasting* 44, no. 3: 286-293.

Schwering, Felix K., Edmond J. Violette, and Richard H. Espeland. 1988. Millimeter-wave propagation in vegetation: experiments and theory. *IEEE Transactions on Geoscience and Remote Sensing* 26, no. 3: 355-367.

Sithole, George and George Vosselman. 2004. Experimental comparison of filter algorithms for bare-earth extraction from airborne laser scanning point clouds. *ISPRS Journal of Photogrammetry and Remote Sensing* 59: 85-101.

Sorensen, Paul A., and David P. Lanter. 1993. Two Algorithms for Determining Partial Visibility and Reducing Data Structure Induced Error in Viewshed Analysis. *Photogrammetric Engineering & Remote Sensing* 59, no. 7: 1149-1160.

Tewari, R. K., S. Swarup, and Mkanujendra Roy. 1990. Radio wave propagation through rain forests of India. *IEEE Transactions on Antennas and Propagation* 38, no. 4: 433-449.

United States Geologic Survey. 2006. Digital Elevation Model (DEM). http://edc.usgs.gov/guides/dem.html (accessed April 25, 2007).

Verma, Vivek, Rakesh Kumar, and Stephen Hsu. 2006. 3D building detection and modeling from aerial LIDAR data. *Proceedings of the IEEE Computer Society*

Conference on Computer Vision and Pattern Recognition, 2213-2220. New York: IEEE Press.

Vogel, Wolfhard J., and Julius Goldhirsh. 1986. Tree attentuation at 869 MHz derived from remotely piloted aircraft measurements. *IEEE Transactions on Antennas and Propagation* 34, no. 12: 1460-1464.

Walfisch, Joram, and Henry L. Bertoni. 1988. A Theoretical Model of UHF Propagation in Urban Environments. *IEEE Transactions in Antennas and Propagation* 36, no. 12: 1788-1796.

Zaksek, Klemen and Norbert Pfeifer. 2006. An improved morphological filter for selecting relief points from a LIDAR point cloud in steep areas with dense vegetation. http://iaps.zrc-sazu.si/files/File/Publikacije/Zaksek_Pfeifer_ ImprMF.pdf (accessed April 25, 2007).

Zhang, Keqi, Shu-Ching Chen, D. Whitman, Mei-Ling Shyu, Jianhua Yan, Chengcui Zhang. 2003. A progressive morphological filter for removing nonground measurements from airborne LIDAR data. *IEEE Transactions on Geoscience and Remote Sensing* 41, no. 4: 872-882.